Spatially Oversampled Demultiplexing in mmWave LoS MIMO

P. Raviteja[(1)] and U. Madhow[(2)]

(1) ECSE Department, Monash University, Clayton, VIC 3800, Australia
(2) ECE Department, University of California, Santa Barbara, CA, USA
Emails: raviteja.patchava@monash.edu, madhow@ece.ucsb.edu

***Abstract*—The transceiver separations required for synthesizing full rank MIMO matrices in line of sight (LoS) geometries scale as the square root of the product of carrier wavelength and range. The wavelengths at millimeter (mm) wave carrier frequencies are small therefore enable LoS spatial multiplexing with practical node form factors at ranges of 10-100 m, depending on the carrier frequency. However, such LoS MIMO links become frequency selective even with small geometric mismatches. Exact channel inversion in an $N \times N$ MIMO system requires fractionally spaced equalization, which is practically infeasible when operating at the very high data rates (multiple Gbps) that we are interested in. In this paper, we investigate spatial oversampling (more receive antennas than transmitted data streams) with symbol rate sampling, introducing *designed* delay diversity across different receive antennas, as a means for removing error floors when linearly separating the spatially multiplexed streams. We study the tradeoff between the number of additional receive antennas and the complexity of temporal equalization, and argue that an attractive example architecture, compatible with form factor constraints, is one in which the number of receive antennas is double the number of transmitted data streams.**

***Index Terms*—mmWave, MMSE equalizer, spatial multiplexing, sampling offset**

I. Introduction

mmWave communication has the potential of providing wireless data rates approaching those of optical links by virtue of two key properties. First, the amount of bandwidth available typically scales linearly with the carrier frequency, so that we might, for example, have 10-20 GHz of bandwidth for a link operating at a carrier frequency over 100 GHz. Second, due to the tiny carrier wavelength, it becomes possible to obtain spatial multiplexing over point-to-point links (i.e., without requiring rich scattering) with transceiver spacings that are small enough to be accommodated in nodes of compact form factor. Roughly speaking, for two-dimensional arrays occupying areas A_t at the transmitter and A_r at the receiver, the MIMO channel rank is approximately $r = \frac{A_t A_r}{(\lambda R)^2}$, where λ denotes carrier wavelength and R the link range. Furthermore, full channel rank can be attained by a sparse array, spacing r elements (each element can itself be a directive array) uniformly over the given area. Thus, for fixed form factor, link range and spectral efficiency, the data rate can scale as f_c^3, where $f_c = \frac{c}{\lambda}$ denotes the carrier frequency: a factor of f_c^2 due to spatial multiplexing, and a factor of f_c due to the linear scaling of bandwidth with f_c.

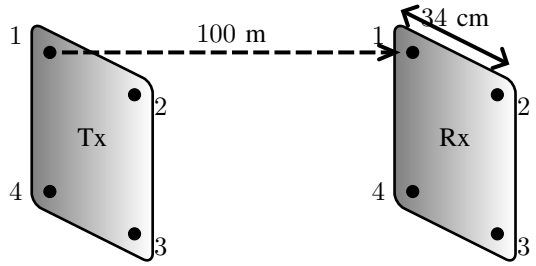

Fig. 1. LoS MIMO system with 4-fold spatial multiplexing

Our work here is motivated by systems such as the example depicted in Figure 1, which shows 4-fold spatial multiplexing using 2D arrays at each end, with link speed exceeding 100 Gbps. Such systems have been considered in [7], [8], where it is pointed out that even small geometric misalignments result in channel dispersion, which leads to error floors with conventional linear space-time equalization with symbol-rate sampling at each receive element. Given the large bandwidth, sampling beyond the symbol rate to implement fractionally spaced equalization is unattractive. The solution proposed in [7] is to employ an analog architecture, using programmable delays with sub-symbol precision to compensate for the dispersion caused by geometric misalignments, while maintaining symbol rate sampling at each receive element. In this paper, we investigate an alternative architecture for space-time linear equalization, compatible with both digital and analog realizations, which employs *spatial* oversampling while maintaining symbol rate sampling. From the point of view of hardware realization, a key advantage is that additional receive elements and associated circuits can easily fit within the same form factor, given that the original set of elements must be widely spaced (as measured in carrier wavelengths) in order to provide the required spatial degrees of freedom. Our main goal in this paper is to demonstrate that such an architecture does eliminate performance floors using linear space-time equalizers of finite complexity, and to explore tradeoffs between complexity and the amount of spatial oversampling. A sweet spot, for example, is to replace each receive element by a pair of elements whose sampling times are offset by $T/2$, which provides enough "delay diversity" to enable separation of the multiplexed streams using a relatively small time domain window (e.g.,

5 samples).

The rich scattering environments assumed in classical spatial multiplexing [2] do not apply over mmWave channels [1]. Basic theoretical tradeoffs in LoS mmWave MIMO are explored in [3], while LoS MIMO for prototype 60 GHz systems with two and four spatially multiplexed streams have been demonstrated in [4] and [5], respectively. Optimal antenna placement, with respect to maximizing mutual information, based on a 3D geometrical model is considered in [6]. As mentioned, we are motivated here by recent work [7], [8] aimed at pushing LoS MIMO bandwidths beyond 10 GHz, where small geometric perturbations lead to frequency selectivity. While [7] considers programmable analog subsymbol delays to undo the effect of such perturbations, our proposed architecture is more flexible: it is compatible with both digital and analog implementations. While our performance evaluation here is focused on the impact of geometric misalignments, the proposed architecture provides enough degrees of freedom to accommodate more general models for frequency selectivity (e.g., due to larger geometric perturbations that might be caused by reflections).

The rest of the paper is organized as follows. The system model is introduced in Sec. II. In Sec. III, we derive the conditions on the channel matrix to avoid error floors, which guides design choices in our proposed architecture. Simulation results are presented in Sec. IV. Sec. V contains our conclusions.

We use the following notation throughout this paper: a, $\mathbf{a}$, and $\mathbf{A}$ represents a scalar, vector, and matrix respectively. $\mathbf{I}_M$ is the identity matrix of size $M \times M$. $\mathbf{A}^T$, $\mathbf{A}^H$, and $\mathbf{A}^{-1}$ denotes the transpose, Hermitian transpose, and inverse of $\mathbf{A}$ respectively. The m^{th} element of $\mathbf{a}$ is represented using $\mathbf{a}[m]$ and the $(m,n)^{th}$ element of $\mathbf{A}$ is $\mathbf{A}[m,n]$.

II. System Model

We first review some LoS basics [3]. While we are interested in 2D arrays in order to maximize spatial multiplexing gain within a compact form factor, consider first LoS spatial multiplexing for a linear array at each end with N transmit and N receive elements, with inter-element spacing of d and R the distance between transmitter and receiver. Assuming ideal alignment, the received signal $\mathbf{y} \in \mathbb{C}^{N\times 1}$ can be written as

$$\mathbf{y} = \mathbf{H}\mathbf{x} + \mathbf{n}, \tag{1}$$

where $\mathbf{x} \in \mathbb{C}^{N\times 1}$ is the transmitted signal vector, $\mathbf{H} \in \mathbb{C}^{N\times N}$ is the channel matrix, and $\mathbf{n} \in \mathbb{C}^{N\times 1}$ is additive white Gaussian noise with covariance matrix $\sigma^2\mathbf{I}_N$. For $R \gg d$, the $(m,n)^{th}$ entry of $\mathbf{H}$ is well approximated as

$$\mathbf{H}[m,n] = \exp\left(-j\pi(m-n)^2\frac{d^2}{\lambda R}\right). \tag{2}$$

This is obtained simply by computing phase differences corresponding to the path length differences for different pairs of transmit and receive elements. (Differences in path loss are negligible.)

Full channel rank and no inter-stream interference is obtained if the columns of $\mathbf{H}$ are orthogonal. This is obtained if we choose the spacing to be [3]

$$d = \sqrt{\frac{R\lambda}{N}}, \text{ or } \frac{d}{\lambda} = \sqrt{\frac{R}{\lambda N}} \tag{3}$$

This provides ideal N-fold spatial multiplexing. By creating a 2D array at each end with N^2 elements arranged in uniform rectangular grid with spacing d, we obtain ideal N^2-fold spatial multiplexing. Typical spacings for attaining full channel rank are large multiples of the wavelengths, unlike the $\lambda/2$-spacing typical in a beamforming array. Thus, each "element" in a LoS MIMO array might be an electronically steerable beamforming "subarray" with sub-wavelength element spacing, or a highly directive fixed beam antenna.

Running example: For $N = 2$ (i.e., 4-fold spatial multiplexing) at a carrier frequency 130 GHz and a range of 100 m, we obtain $d = 34$cm from (3), which is almost 150λ. Using parameters from [7], [8], a bandwidth of 20 GHz using QPSK yields an uncoded data rate of 160 Gbps, assuming no excess bandwidth, which implies that data rates exceeding 100 Gbps are enabled by such architectures, even when accounting for excess bandwidth and lightweight channel coding.

Now, we consider the effect of geometric misalignments, when the transmit and receive arrays are slightly tilted with respect to each other [7], [8]. At 20 GHz symbol rate, even a small tilt angle of 7.5° can yield a 3 symbol channel delay spread, creating an FIR space-time channel rather than the ideal spatial channel model in (1). We therefore consider space-time linear equalization, with each symbol decision involving samples from a time window of length W symbols from all the receive elements.

In principle, it is possible to handle frequency selectivity using standard techniques such as OFDM or frequency domain equalization. However, given the large bandwidths, implementations of the FFT or IFFT operations associated with such techniques become unattractive. For the short channels arising in our context, single carrier modulation with time domain equalization has significantly lower computational complexity.

Considering linear arrays at each end for simplicity of exposition, and now allowing a possibly different number of transmit and receive elements, denoted by N_t and N_r, respectively, the received signal over a window of length W is given by

$$\widetilde{\mathbf{y}} = \widetilde{\mathbf{H}}\widetilde{\mathbf{x}} + \widetilde{\mathbf{n}}, \tag{4}$$

where

$$\begin{aligned}
\widetilde{\mathbf{y}} &= \begin{bmatrix}\mathbf{y}_K^T & \mathbf{y}_{K-1}^T & \cdots & \mathbf{y}_{K-W+1}^T\end{bmatrix}^T \in \mathbb{C}^{N_rW\times 1} \\
\widetilde{\mathbf{H}} &= \begin{bmatrix}\mathbf{H}_0 & \cdots & \mathbf{H}_{L-1} & \cdots & \mathbf{0} & \mathbf{0} \\ \mathbf{0} & \mathbf{H}_0 & \cdots & \mathbf{H}_{L-1} & \cdots & \mathbf{0} \\ \vdots & \ddots & \ddots & \ddots & \ddots & \vdots \\ \mathbf{0} & \mathbf{0} & \cdots & \mathbf{H}_0 & \cdots & \mathbf{H}_{L-1}\end{bmatrix} \\
\widetilde{\mathbf{x}} &= \begin{bmatrix}\mathbf{x}_K^T & \mathbf{x}_{K-1}^T & \cdots & \mathbf{x}_{K-L-W+1}^T\end{bmatrix}^T \in \mathbb{C}^{N_t(L+W-1)\times 1} \\
\widetilde{\mathbf{n}} &= \begin{bmatrix}\mathbf{n}_K^T & \mathbf{n}_{K-1}^T & \cdots & \mathbf{n}_{K-W+1}^T\end{bmatrix}^T \in \mathbb{C}^{N_rW\times 1}
\end{aligned} \tag{5}$$

Here, $\mathbf{x}_k \in \mathbb{C}^{N_t \times 1}$ and $\mathbf{y}_k \in \mathbb{C}^{N_r \times 1}$ are the transmitted and received signals at time kT_s respectively, where T_s is the sampling time, $\widetilde{\mathbf{H}} \in \mathbb{C}^{N_r W \times N_t(L+W-1)}$ is a block Toeplitz matrix, and $\mathbf{H}_l \in \mathbb{C}^{N_r \times N_t}, l \in [0, L-1]$ denote the L-tap frequency selective channel. The $(m,n)^{th}$ entry of $\mathbf{H}_l$ is

$$\mathbf{H}_l[m,n] = \sqrt{\frac{1}{N_t}} \exp\left(-j\pi(m-n)^2 \frac{d^2}{\lambda R}\right) \exp(-j2\pi f_c(\mu_m + \tau_n)) p(lT_s - \mu_m - \tau_n), \quad (6)$$

where, $\sqrt{\frac{1}{N_t}}$ is the normalization factor, the term $\exp\left(-j\pi(m-n)^2 \frac{d^2}{\lambda R}\right)$ represents the channel gain without misalignment, μ_m and τ_n are the additional delays occurred at the receiver m and the transmitter n respectively, and $p(t)$ is the transmitted pulse. In the next section, we study the linear equalizer for the system in (4).

The block Toeplitz structure naturally also holds for 2D arrays at each end, but the detailed specification of the channel matrix is messier, and is therefore omitted. Our numerical results, however, are for 2D arrays.

III. Linear Space-Time Equalizer

The space-time equalizer considers the received signals at N_r receive antennas over a time duration of W symbol intervals, and estimates N_t transmitted symbols in which every symbol is from a different transmit antenna. Then the space-time window slides by one symbol to estimate the next N_t transmitted symbols. We assume that the receiver knows the channel $\widetilde{\mathbf{H}}$.

General criteria for the existence of finite-complexity linear space-time zero-forcing (ZF) equalizers are provided via the generalized Bezout identity [9], which states that $\widetilde{\mathbf{H}}(Z)$ (the z-domain representation of $\widetilde{\mathbf{H}}$) must be right co-prime. However, we find that detailed design insights are easier to obtain by working in the time domain.

For a given time window of length W, we must choose the N_t decoded symbols, one for each transmitted stream, from among the $N_t(L+W-1)$ transmitted symbols contributing to the received samples in the window, as shown in (4). Let us denote the positions of the decoded N_t transmitted symbols by $\Gamma_s, s \in \{0, 1, \cdots, N_t - 1\}$ and $\Gamma_s \in \{iN_t + s; i \in \{0, 1, \cdots, L+W-2\}\}$. We employ a simple heuristic for selecting the values of Γ_s: for each transmitted stream, choose the symbol with the maximum energy contributed to the current window of space-time samples:

$$\Gamma_s = \underset{j=iN_t+s; i\in\{0,1,\cdots,L+W-2\}}{\arg\max} \|\widetilde{\mathbf{H}}_j\|^2, \quad (7)$$

where $\widetilde{\mathbf{H}}_j$ is the j^{th} column of $\widetilde{\mathbf{H}}$.

The ZF equalizer satisfies

$$\widetilde{\mathbf{c}}^s \widetilde{\mathbf{H}} = \begin{bmatrix} \mathbf{0}_{1\times(\Gamma_s-1)} & 1 & \mathbf{0}_{1\times N_t(L+W-1)-\Gamma_s} \end{bmatrix}, \quad (8)$$

where $\widetilde{\mathbf{c}}^s = \begin{bmatrix} \mathbf{c}_0^s & \cdots & \mathbf{c}_{W-1}^s \end{bmatrix}$, $\mathbf{c}_l^s \in \mathbb{C}^{1\times N_r}, l \in \{0, \cdots, W-1\}$ is the linear weight vector to decode the symbol transmitted from s^{th} antenna.

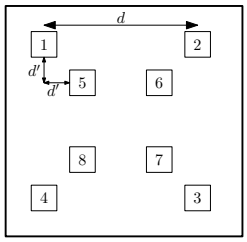

Fig. 2. 2X spatial oversampling within the same form factor.

A sufficient condition for a solution to exist for (8) is given by the following lemma.

Lemma 1: The ZF weight vector $\mathbf{c}^s$ can always be found if the following conditions are satisfied:

1) $N_r \geq N_t$
2) The window length

$$W \geq W_0 = \left\lceil \frac{L-1}{\left(\frac{N_r}{N_t}\right) - 1} \right\rceil \quad (9)$$

3) $\widetilde{\mathbf{H}}$ has full column rank

Proof: The condition in (8) is a linear system of equations with $N_r W$ unknowns and $N_t(L+W-1)$ equations. A nontrivial solution exists if the number of unknowns is greater than or equal to the number of equations, and if $\widetilde{\mathbf{H}}$ is full rank. This is possible if $N_r \geq N_t$ and

$$N_r W \geq N_t(L+W-1)$$
$$W \geq W_0 = \left\lceil \frac{L-1}{\left(\frac{N_r}{N_t}\right) - 1} \right\rceil$$

■

The conditions in Lemma 1 satisfy the criteria in Theorem 2 of [9]. However, unlike at lower carrier frequencies, we cannot rely on rich multipath to satisfy the full rank condition. In the next subsection, we propose the use of sampling offsets across receivers to satisfy this condition.

A. Spatially oversampled reception

Starting with N^2-fold spatial multiplexing with d-spaced 2D arrays, we propose to add receive elements on the "inside" of the array, so that we do not increase the overall area occupied by the array. Recognizing that each element may itself be a subarray, the new receive elements must be placed many wavelengths away from the original elements. The output of each receive element is sampled at the symbol rate, but in order to provide a "different enough view" of the physical channel via the additional elements, we may need to sample them at an offset from those in the original elements.

An example of the proposed architecture at the receiver is given in Fig. 2. In this figure, receivers 1 through 4 are the original antennas, separated at a distance d that provides full spatial rank, while the additional receivers 5 through 8

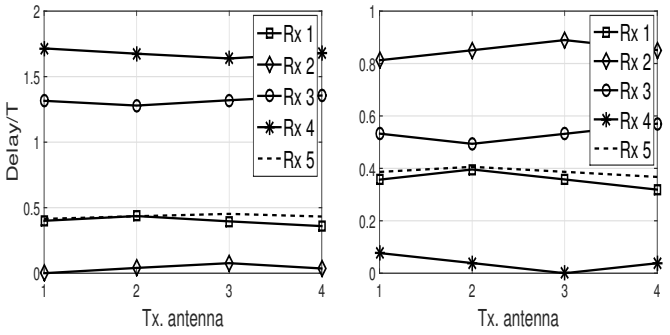

Fig. 3. The variation of delays at the different receive antennas

provide spatial oversampling. Here d' can be set to $d/4$ to get the maximum separation among the receivers within the original form factor. It is important to sample the additional receivers at an offset ($T/2$ being a good choice) from the original receivers in order to achieve full rank. To see this, we plot in Fig. 3 the delays incurred by different transmitters at the receivers (as a multiple of symbol time T) for two different small misalignments. The values of d, λ, R, and T(50 ps) are as in the running example. We observe that the delays at the additional receiver 5 are close to those at the nearest original receiver 1, and hence so are the channels. We therefore sample the additional receivers at an offset of $T/2$ in order to ensure that the full rank condition is satisfied.

While the preceding approach is intuitively pleasing for $N_r = 2N_t$, optimizing placement and sampling offsets for more general settings is an interesting problem for future investigation.

B. MMSE Equalizer

While the ZF equalization condition guides our architecture, in order to account for noise, our performance evaluations consider the MMSE equalizer, which minimizes $\mathbb{E}\left[\| \left(\widetilde{\mathbf{c}}^s\right)^H \widetilde{\mathbf{y}} - \widetilde{\mathbf{x}}[\Gamma_s]\|^2\right]$ for the sth input stream.

$$\widetilde{\mathbf{c}}^s_{\text{MMSE}} = \left(\widetilde{\mathbf{H}}\widetilde{\mathbf{H}}^H + (\sigma^2/P)\mathbb{I}_{N_rW}\right)^{-1}\widetilde{\mathbf{H}}_{\Gamma_s}, \qquad (10)$$

where P is the signal power at each transmit antenna. The decision statistics for the N_t transmitted input symbols are then given by

$$\hat{\mathbf{x}}_{\text{est}} = \left(\widetilde{\mathbf{c}}^s_{\text{MMSE}}\right)^H \widetilde{\mathbf{y}}. \qquad (11)$$

C. Trade-off between W and N_r

The time window W_0 for equality in (9) is a decreasing function of the number of receivers N_r, assuming that the number of data streams N_t and the channel length L are fixed. From (11), we see that the number of complex-valued operations per transmitted symbol for MMSE demodulation is given by N_rW_0. This actually decreases as N_r increases, as we see from the equality condition in (9):

$$N_rW_0 = N_t(L-1) + N_tW_0.$$

Table I shows the trade-off between N_r and W_0 with $L = 6$ and $N_t = 4$ LoS MIMO system.

TABLE I
TRADE-OFF BETWEEN N_r AND W_0 FOR $L = 6$ AND $N_t = 4$

N_r	5	6	7	8
W	20	10	7	5

IV. SIMULATION RESULTS

In this section, we simulate the average SINR and BER of the proposed system for different window lengths and sampling offsets. We consider the LoS system in Fig. 2 and the parameters d, λ, and R as in the running example. We generate the additional delays μ_m and τ_n by assuming small random rotations (less than 5°) at the transmitter and receiver. Each data stream uses QPSK modulation with a raised cosine pulse $p(t)$ with roll-off factor 0.25. The SINR of the s^{th} stream is computed as

$$\text{SINR}_s = \frac{\left|\widetilde{\mathbf{c}}^s_{\text{MMSE}}\widetilde{\mathbf{H}}_{\Gamma_s}\right|^2}{\sum_{i\neq\Gamma_s}\left|\widetilde{\mathbf{c}}^s_{\text{MMSE}}\widetilde{\mathbf{H}}_i\right|^2 + \frac{\sigma^2}{P}\left|\left(\widetilde{\mathbf{c}}^s_{\text{MMSE}}\right)^H\widetilde{\mathbf{c}}^s_{\text{MMSE}}\right|^2}.$$

In order to obtain BER estimates, we run the simulations until we see 500 errors and at least 10^4 different channel realizations. We define SNR as P/σ^2, the (SISO benchmark) SNR per receive antenna for a given transmitted stream.

Figs. 4 and 5 show the SINR and BER of the proposed oversampled system for different window lengths of $W_0, W_0/2, 3W_0/4$, and $2W_0$ with $N_r = 8$ and $N_t = 4$, where W_0 denotes the window length for equality in (9). The additional receive antennas (5-8) are sampled at an offset of $T/2$ from the main antennas. The benchmarks associated with the original system ($N_r = 4$) are for ideal alignment as in (1), as well as with geometric misalignments. In the latter setting, the channel is not invertible using an FIR equalizer, but we still limit the time window to 4 in order to compare performance with limited computational complexity. From these figures, we observe that i) all of the systems with $N_r = 8$ perform better than the system with $N_r = 4$; ii) performance improves with window length until W_0 and saturates thereafter; iii) the performance of $W = W_0$ and $N_r = 8$ has no error floors and is about 2 dB better than ideal alignment system with $N_r = 4$.

We conclude that, while a window length of W_0 is necessary to avoid error floors, the noise enhancement is small enough at $W = W_0$ that (a) further increases in temporal complexity do not help, (b) the 3 dB improvement due to noise averaging implies that a misaligned system with $N_r = 8$ performs better than an ideally aligned system with $N_r = 4$.

Figs. 6 and 7 plot the SINR and BER for $N_r = 8$ and $W = W_0$, showing that no sampling offsets at the additional receivers leads to error floors, unlike the proposed offsets of $T/2$. This behavior is explained by the full rank condition on $\widetilde{\mathbf{H}}$ in Lemma 1.

V. CONCLUSION

We have shown that spatial oversampling, along with designed delay diversity, is an effective approach to combat the frequency selectivity caused by geometric misalignments in

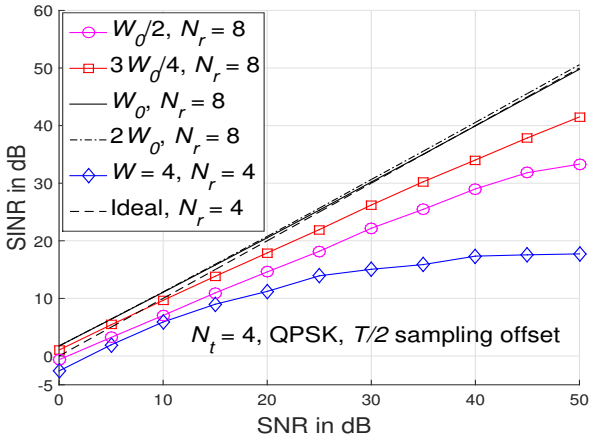

Fig. 4. SINR of the proposed oversampled LoS MIMO system for different window lengths with $N_t = 4$ and QPSK

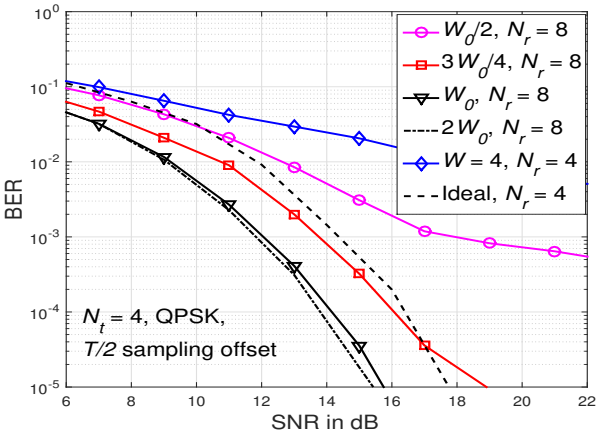

Fig. 5. BER of the proposed oversampled LoS MIMO system for different window lengths with $N_t = 4$ and QPSK

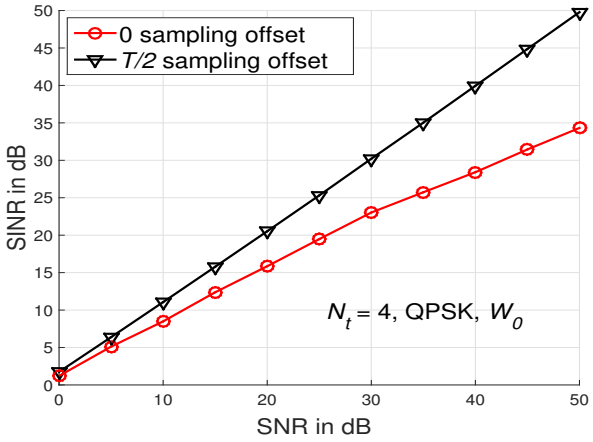

Fig. 6. SINR of the proposed oversampled LoS MIMO system for different sampling offsets at extra receive antennas with $N_t = 4$ and QPSK

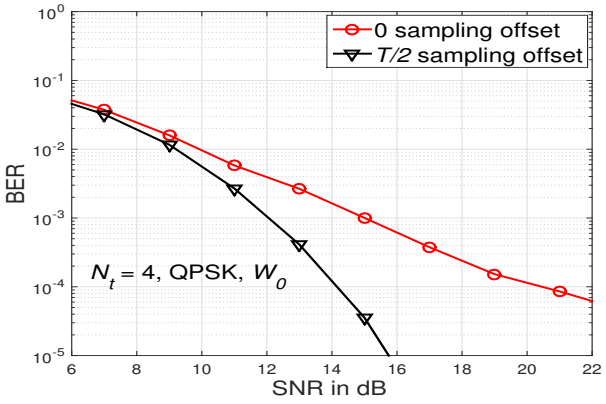

Fig. 7. BER of the proposed oversampled LoS MIMO system for different sampling offsets at extra receive antennas with $N_t = 4$ and QPSK

LoS MIMO. A time-domain zero-forcing condition is used to identify the tradeoff between the number of additional receivers and the equalizer time window, and a particularly attractive architecture is to double the number of receivers within the same form factor. An important topic for future work is to investigate tradeoffs between all-digital and hybrid analog-digital implementations of such architectures.

VI. Acknowledgement

This work was supported in part by the US National Science Foundation under grant CNS-1518812, and by a gift from Facebook, and by the Graduate Research International Travel Grant of the Faculty of Engineering at Monash University.

References

[1] T. S. Rappaport, R. W. Heath Jr., R. C. Daniels, and J. N. Murdock, *Millimeter Wave Wireless Communications.* Englewood Cliffs, NJ, USA: Prentice-Hall, Sep. 2014

[2] G. J. Foschini and M. Gans, "On the limits of wireless communications in a fading environment when using multiple antennas," *Wireless Personal Commun.,* vol. 6, no. 3, p. 311, Mar. 1998.

[3] E. Torkildson, U. Madhow, and M. Rodwell, "Indoor millimeter wave MIMO: Feasibility and performance," *IEEE Trans. Wireless Commun.,* vol. 10, no. 12, pp. 4150-4160, Dec. 2011.

[4] C. Sheldon, E. Torkildson, M. Seo, C. P. Yue, U. Madhow, and M. Rodwell, "A 60GHz line-of-sight 2x2 MIMO link operating at 1.2 Gbps," *in IEEE Antennas and Propagation Society International Symposium,* San Diego, CA, pp. 1-4, July 2008.

[5] C. Sheldon, M. Seo, E. Torkildson, M. Rodwell, and U. Madhow, "Four-channel spatial multiplexing over a millimeter-wave line-of-sight link," *in IEEE MTT-S International Microwave Symposium Digest,* Boston, MA, pp. 389-392, July 2009.

[6] F. Bohagen, P. Orten, and G. Oien, "Design of optimal high-rank line-of-sight MIMO channels," *IEEE Trans. Wireless Commun.,* vol. 6, no. 4, pp. 1420-1425, Apr. 2007.

[7] B. Mamandipoor, M. Sawaby, A. Arbabian, and U. Madhow, "Hardware-constrained signal processing for mmWave LoS MIMO," *in IEEE 49th Asilomar Conference on Signals, Systems and Computers,* pp. 1427-1431, Pacific Grove, CA, Nov. 2015.

[8] M. Sawaby, B. Mamandipoor, U. Madhow and A. Arbabian, "Analog processing to enable scalable high-throughput mmWave wireless fiber systems," *in IEEE 50th Asilomar Conference on Signals, Systems and Computers,* Pacific Grove, CA, pp. 1658-1662, Nov. 2016.

[9] S. Y. Kung, Y. Wu, and X. Zhang, "Bezout space-time precoders and equalizers for MIMO channels," *IEEE Trans. Signal Process.,* vol. 50, no. 10, pp. 2499-2514, Oct. 2002.